VIA MEDICA

ORIGINAL ARTICLE

Folia Morphol.
Vol. 82, No. 4, pp. 898–908
DOI: 10.5603/FM.a2022.0094

ISSN 0015–5659
eISSN 1644–3284
journals.viamedica.pl

A micro-computed tomography study of the sinus tympani variation in humans

J. Skrzat[1], M. Kozerska[1], M. Zarzecki[1], S. Wroński[2], J. Tarasiuk[2]

[1]*Department of Anatomy, Jagiellonian University Medical College, Krakow, Poland*
[2]*Department of Condensed Matter Physics, AGH-UST University of Science and Technology, Krakow, Poland*

[Received: 29 August 2022; Accepted: 16 October 2022; Early publication date: 28 October 2022]

Background: *The posterior part of the tympanic cavity comprises a depression called the sinus tympani (ST). The said structure is of outmost importance, e.g. in surgical procedures involving the middle ear, as a pathology (microbial biofilm or cholesteatoma) present in this difficult to access location might hinder its effective treatment. The aim of the study was to evaluate anatomical variants of the ST in human adult petrous bones. For this purpose, three-dimensional (3D) models of the ST were recreated from micro-computed tomography (CT) scans of 44 dry petrous bone samples (19 female, 25 male), applying 3D Slicer, Meshmixer and MeshLab software.*

Materials and methods: *Anatomical variants of the ST were classified in terms of both shape and surface configuration. The internal configuration of the ST was classified as heterogeneous — containing small bony trabeculae and crests up to 1.0 mm in size, contrasting to homogeneous ST that characterizes a relatively smooth interior, or mere presence of minor depressions and mild folds. Female STs were more bowl-shaped (57.9%) than saccular (42.1%), and had heterogeneous surface configuration (52.6%) compared to homogeneous (47.4%). On the contrary, male STs were more saccular (52.0%) rather than bowl-shaped (48.0%), and predominantly had a heterogeneous surface (84.0%) over homogeneous (16.0%).*

Results and Conclusions: *A complex combination of ST features comprised of a saccular shape and heterogeneous surface occurred in 52.0% of males and in 15.8% of females (a statistically significant difference; $p = 0.0254$, Fisher's exact test) seems to be clinically important because of its potential negative implication on health outcomes after surgery in the case of, for example, cholesteatoma, and it may also favour chronic pathological processes.* (Folia Morphol 2023; 82, 4: 898–908)

Key words: sinus tympani, retrotympanum, middle ear, micro-computed tomography

INTRODUCTION

The sinus tympani (ST) is a depression localized in the retrotympanum (the posterior area of the tympanic cavity) and forms its medial portion. The mean depth of the ST in adults was estimated to be 2.6–2.7 mm, but there are also reports stating that it can reach even up to 10 mm [8, 16, 41]. The ST lies below and posteriorly to the promontory, posteriorly to the round window, extends medially to the pyramidal eminence, stapedial muscle, and facial canal

Address for correspondence: M. Kozerska, PhD, Department of Anatomy, Jagiellonian University Medical College, ul. Kopernika 12, 31–034 Kraków, Poland, e-mail: magdalena.kozerska@uj.edu.pl

(its mastoid segment) and laterally to the posterior semicircular canal [19]. The superior boundary of the ST forms the ponticulus, whereas the subiculum is the inferior boundary. The subiculum is the posterior extension of the promontory that separates the ST from the round window [34].

Many studies have emphasized the clinical importance of the ST because of pathological processes which may occur inside, and highlight difficulties in surgical approaches and endoscopic explorations of this region of the middle ear [5, 7]. One of such pathologies is cholesteatoma that is an abnormal accumulation of keratinized squamous epithelium inside the ear. It has a destructive effect on the auditory structures causing their inflammation that might eventually lead to erosion of the bone. Therefore, a timely treatment is required, involving surgical removal of the cholesteatoma [48].

Epidemiological data revealed that cholesteatomas occur more often in Caucasian than African or Asian populations. The cholesteatoma affects all age groups. The annual incidence of cholesteatoma is estimated to be about 3 per 100,000 in children and about 9 to 12 per 100,000 in adults, with a male predominance (1.4:1) [39]. However, its occurrence has changed over time, and varies across countries showing different annual trends [27, 47]. Moreover, this disease can manifest unilaterally or bilaterally. The bilateral occurrence of cholesteatomas has been found in 10–20% of cases, male children and adolescents are affected more often than females [47].

Although cholesteatoma has been recognised for more than three centuries [20], the nature of this disorder has yet not been fully determined, particularly the factors regulating its progression [28]. Some studies revealed that sex predilection for cholesteatoma might be dependent on the expression of female sex hormone receptors in the middle ear that act as an auditory protectant [43]. It has also been noted that various expression of genes may control pathogenesis of cholesteatomas [3, 29, 40].

Pathophysiological and epidemiological data encourage undertaking various studies aimed at identifying factors that favour implantation of cholesteatoma, and those that restrict its complete removal from the middle ear. It is particularly true for its excision from the ST which is regarded as the so-called "hidden structure in the ear," and endoscopic and surgical access to its interior can be troublesome. Therefore, detailed three-dimensional (3D) presentation of the ST topography and anatomy may enhance perspectives in treating cholesteatoma, which often invades this part of the middle ear.

In the recent years, high-resolution computed tomography (CT) and endoscopic examinations have been used to show the internal anatomy of the ear [14, 15]. These imaging techniques allow to perceive morphological changes related to the ear pathologies or structural malformations important from the clinical point of view. Notwithstanding, some anatomical details can be omitted in visual assessment or hardly recognised due to limited spatial imaging attained in clinical tomography or due to limited field of view during an endoscopic inspection.

In pre-clinical studies such technical limitations of viewing anatomical structures in detail can hinder appropriate evaluation of the morphological variants, especially if their dimensions are in range of a millimetre or even less. Formerly, only manual sectioning of the ear could reveal the entire spectrum of its morphological details and varieties [25]. Nowadays, this tedious and time consuming procedure has been substituted by the micro-computed tomography (micro-CT) which delivers images with microscopic precision. Hence, series of the micro-CT scans allows to perform 3D reconstructions of the studied samples and to section them virtually in order to display their internal morphology [18, 44].

Therefore, in the present study the authors applied micro-CT imaging of the ST, so as to display its anatomy in the 3D mode. The said approach facilitated multidirectional viewing and comparison of its morphological features, allowing for their subsequent assessment and classification of possible variations.

MATERIALS AND METHODS

Three-dimensional imaging of the ST was performed on 44 adult temporal bones (25 male and 19 female of Caucasian origin) whose age at death ranged from 30 to 70 years. The examined bones have been dated back to the XVIIth century. In order to obtain the temporal bones, we used fragmented human skulls found during archaeological excavations conducted in the Southern Poland that were deposited in the Department of Anatomy of the Jagiellonian University Medical College. Henceforth, no skulls were neither deliberately damaged nor destroyed in order to conduct the present study. The specimens were well preserved and did not show any pathological

changes, nor deformations that would exclude them from the present study.

The petrous part was cut off from each temporal bone and scanned with micro-CT using a Nanotom 180N equipped with 180 kV/15 W ultra-high performance nanofocus X-ray tube, with set parameters: I = 250 μA and V = 70 kV (GE Sensing & Inspection Technologies Phoenix X-ray Gmbh). The tomograms were registered on a Hamamatsu 2300 × 2300 pixel detector.

The reconstructions of the scanned specimens were created with the aid of the GE software datosX ver. 2.1.0 using the Feldkamp algorithm [22]. The obtained micro-CT scans had dimensions of 1796 × × 2284 × 1100 pixels, whereas the image pixel size was 18.6 μm. The post-reconstruction data processing included: denoising, cropping and 16 to 8 bit conversion, performed by the means of the VGStudio Max 2.1 software (https://www.volumegraphics.com).

In order to obtain stand alone 3D models of the ST, serial micro-CT scans of the petrous bone images representing the retrotympanum were segmented with the help of the thresholding algorithm. This procedure was performed with the aid of the 3D Slicer software (https://www.slicer.org) which is a free, open source package dedicated for medical and biomedical applications [21].

In the next step, the Autodesk Meshmixer free software (https://www.meshmixer.com) was used for virtual extraction of the ST from the retrotympanum and other anatomical structures included in the initial 3D model of the petrous bone. Such pre-prepared 3D models of the retrotympanum with the ST were displayed on the computer screen and processed interchangeably by the means of Meshlab and Meshmixer software to obtain isolated 3D models of the ST. Using clipping planes and tools dedicated for virtual cutting of the 3D models, the authors removed these parts of the model which occluded the ST. The MeshLab software (https://www.meshlab.net) was indispensable for accomplishing the 3D model of the ST represented by the mesh of triangles, stored in the STL file format [17].

With the aid of the MeshLab software, the authors decimated and smoothed the original mesh of triangles representing the retrotympanum which was further used for creating the final 3D model of the ST. Mesh decimation reduces the number of vertices, edges, and triangles in a mesh, thus the file including 3D model attains smaller size and can be processed quicker by the computer software [6]. Decimation was necessary because the original meshes approximating geometrical configuration of the entire retrotympanum consisted of a huge number of triangles (in the order of 10 million) which tremendously effected the size of the STL files. In our material, the size of the original STL files ranged approximately from 300 Mb to 500 Mb, whereas decimated meshes by half yielded twice smaller files but still preserved the mesh's topology. To simplify the initial mesh of the triangles we applied quadratic edge collapse decimation strategy implemented in the MeshLab software [24]. Thus, the target meshes representing standalone 3D models of the ST usually comprised 20,000–100,000 triangles, depending on the volume of the ST.

The mesh smoothing reduced noise in the model surface and resulted in a more user friendly visual perception. For this purpose, the authors applied the Laplacian smoothing algorithm which creates a new mesh according to local information on the position of the vertexes in the mesh [32]. However, this operation was taken with the outmost precaution, because the smoothing algorithm may inadvertently alter the surface properties of the object and shrink the mesh. To prevent the unwanted changes of the mesh geometry, the authors experimentally adjusted the smoothing force at each iteration applied for mesh processing and compared the changes with reference to the original mesh topology. This was a crucial step in the present study in order to obtain reliable results of visual observations of the ST's interior. Overly smoothened model may erroneously reflect geometrical and morphological properties of the anatomical structures due to extreme elimination of tiny elements like spikes, folds or depressions which naturally exist on the ST's surface.

The process of creating 3D models used for evaluation ST's morphology has been visualized in the flowchart (Fig. 1).

By rotating the 3D models and viewing the ST at different angles on the computer screen, the authors evaluated resemblance of their shapes to geometrical figures. In truth, the shapes reflected by the 3D models should be considered to be virtual endocasts of the STs.

Surface configuration of the ST's interior was evaluated visually with reference to the material texture (smooth — homogeneous, rough — heterogeneous). Outstanding features characteristic for the ST configuration were measured on the 3D models by means of the ruler tool available in the MeshLab software.

The occurrence of each anatomical variant of the ST was estimated as the percentage of the defined

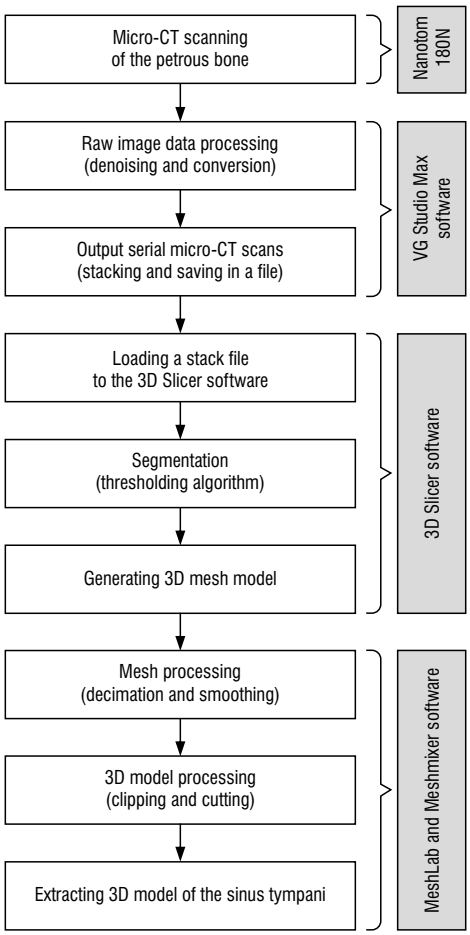

Figure 1. The flowchart of the three-dimensional (3D) model generation from micro-computed tomography (CT) scans.

types in the whole data set, determined separately for the female and male temporal bones. Statistical analysis was completed using a Fisher's exact test processed with the Statistica package ver. 13 (https://www.statsoft.pl). The level of statistical significance for the results was set at $p < 0.05$.

Ethical consideration

The study was conducted with approval (KBET/198/B/2014) of the Bioethics Committee of the Jagiellonian University.

RESULTS

For better orientation in the ST topography, the authors present a representative 3D model showing the location of the ST in relation to the surrounding osseous structures of both the middle and inner ear (Fig. 2).

Regarding the shape of the ST, the authors distinguished two basic morphological forms that were regarded as saccular or bowl. The saccular shaped ST characterizes postero-inferior elongation. This means that one of its diameters is considerably bigger than the other two. In turn, the bowl shaped ST resembles an irregular ovoid, in which three dimensions are similar (Fig. 3). The authors also found that the bowl shaped STs were usually wide and relatively shallow compared to the saccular types of the STs which were sitted deeply in the retrotympanum. The saccular STs

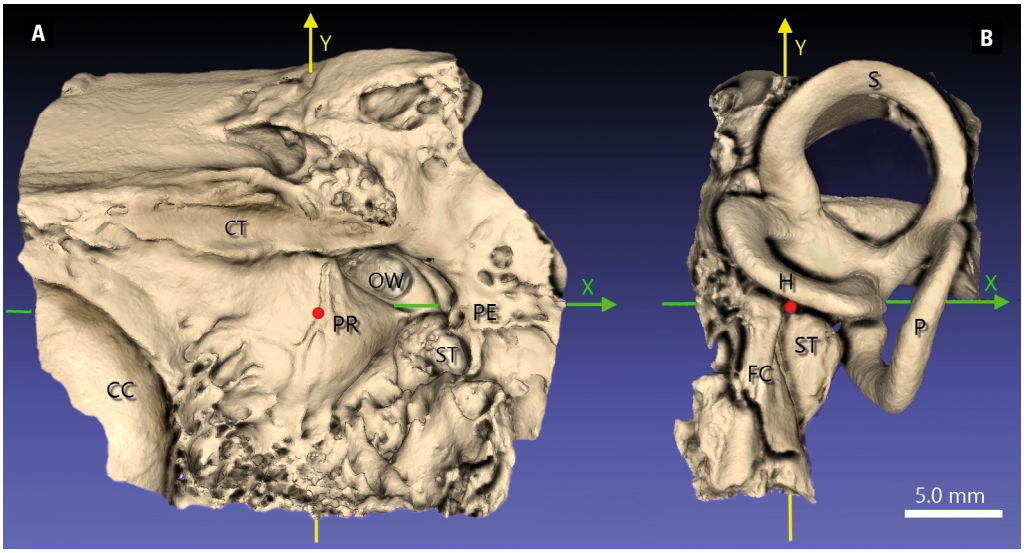

Figure 2. A. A three-dimensional model of the retrotympanum showing the location of the sinus tympani (ST) seen in the medial projection; CC — carotid canal; CT — canal of tensor tympani muscle; PR — promontory; OW — oval window; PE — pyramidal eminence; **B.** The same model rotated clockwise along the Y-axis; wall of the ST bulges posteriorly in the close proximity to the facial canal (FC) and semicircular canals: horizontal (H), posterior (P), superior (S). Orientation of the XYZ coordinate system follows as: the X-axis runs between the lower edge of the OW and the superior edge of the opening to the ST, the Y-axis corresponds to the descending portion of the FC, the Z-axis passes through the promontory (red point), perpendicularly to the X-Y axis.

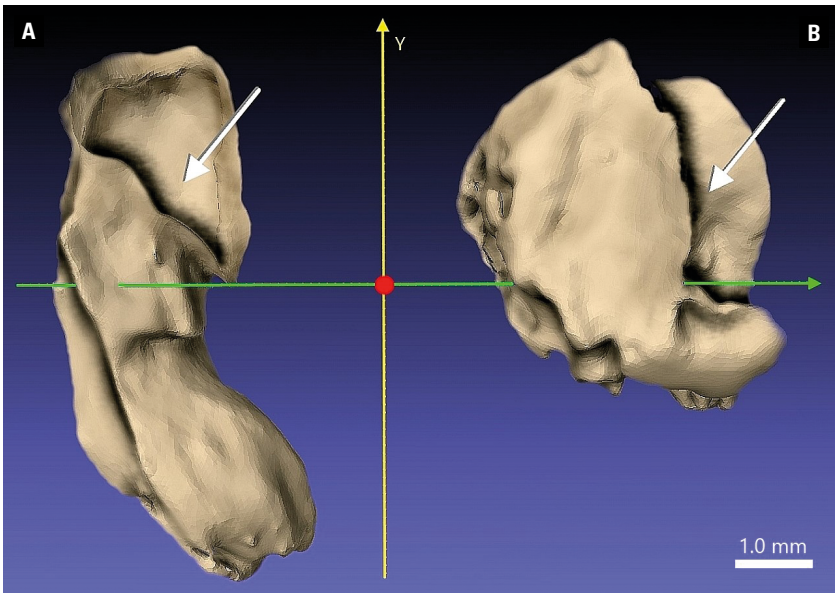

Figure 3. Three-dimensional models of the sinus tympani being of distinct shape: the saccular (**A**) and the bowl (**B**); the arrows indicate the entry to the interior of the sinus tympani.

were usually cylindrical in shape, except for a singular case in which a form, reseambling triangular pyramids (tetrahedra) of variable size, was noted (Fig. 4).

Regardless of the shapes of the STs, their interior structure revealed variable configuration which was defined as homogeneous or heterogeneous, depending on the presence or absence of tiny bony structures located in their walls (Fig. 5). The irregular bony structures found in the heterogeneous STs looked like: trabeculae, crests or laminae with diameters of around 1.0 mm. It should be noted that some of the heterogeneous STs were characterised by the presence of recesses or diverticula emerging from their walls. Such structural modifications were chiefly found in the saccular type of the STs. However, their existence was not included in the STs classification because their size and configuration did not affect the overall shape of the ST.

In turn, homogeneous configuration was attributed to these STs in which their interior was relatively smooth. Their walls were characterized by the lack of bony protrusions. Nonetheless, in some of them mild folds and depressions or pits were observed.

The present study demonstrated that both the saccular and bowl-shaped STs had a similar prevalence (47.7% and 52.3%, respectively) in the combined sex analysis. Furthermore, the authors did not find significant differences between the occurrence of these shapes in the male and female subgroups (Fisher's exact test, $p = 0.557$). As for the internal characteristics of the ST, the heterogeneous surface was typical for the entire sample (70.5%), whereas homogeneous surface was less common with respect to all the samples (29.5%); however, almost half of the female subgroup (47.4%) was characterized with the latter type of the ST. Although male STs were largely heterogeneous (84.0%), their prevalence just about predominated in females (52.6%). The differences in prevalence of the homogeneous and heterogeneous surfaces of the STs in male and female subgroups were statistically significant (Fisher's exact test, $p = 0.044$). The percentage of all observed morphological variants of the ST in male and female subgroups are graphed in Figure 6 and presented in Table 1.

Finally, the authors estimated the number of cases in which the ST revealed a combination of the following morphological features: saccular shape and heterogeneous surface. Such a complex anatomy may hinder surgical operations and lead to pathological processes by facilitating the harbouring of pathogens. Among all the examined sinuses, 36.4% involved this specific anatomy (Table 2). However, the said combination occurred in 13 out of 25 male samples (52.0%), whereas only 3 out of 19 (15.8%) female samples had this composition, a statistically significant difference (Fisher's exact test, $p = 0.025$).

DISCUSSION

So far, morphological variation of the ST has been evaluated utilising either CT or endoscopic images, or dissected temporal bones. Therefore, its evaluation

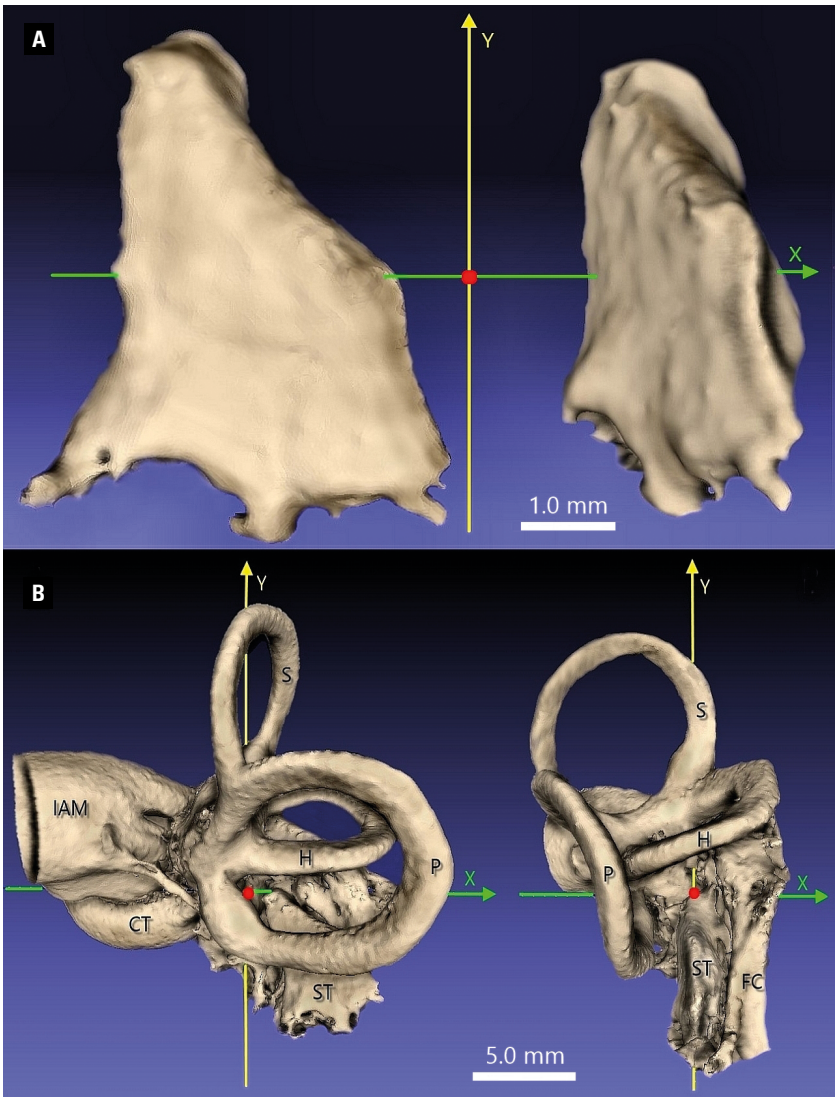

Figure 4. A. The three-dimensional (3D) model of the specific saccular type of sinus tympani (ST) resembling a tetrahedron in shape, seen in both lateral and posterior projection; **B.** A 3D model displaying topography of the ST in reference to the semicircular canals: posterior (P) — horizontal (H), superior (S) and the facial canal (FC); the cochlear turn (CT) and the internal acoustic meatus (IAM) were also identified.

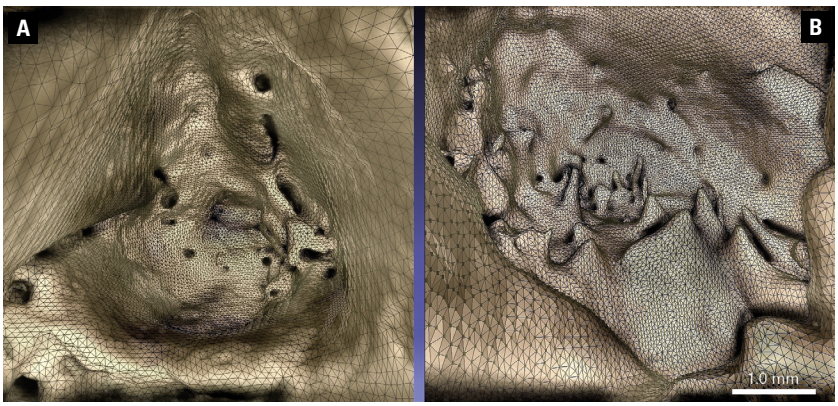

Figure 5. Three-dimensional models showing different internal characteristics of the sinus tympani (ST), approximated by the mesh of triangles; **A.** Homogeneous configuration of the ST. The inner surface is relativly smooth. It is possible to notice tiny pits and small pockets; **B.** Heterogeneous configuration of the ST. The inner surface is rough and irregular; bony spikes, protuberances and creases protrude from the wall of the ST into its lumen, therefore resemble small hillocks and valleys.

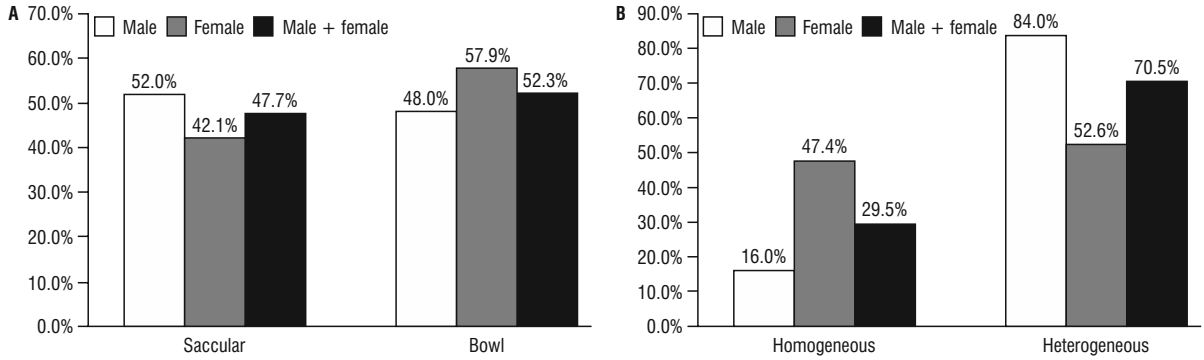

Figure 6. Percentage values of the morphological variants of the sinus tympani, classified according to shape (**A**) and surface (**B**) configuration in male and female temporal bones, respectively.

Table 1. Percentage of the morphological variants of the sinus tympani

Sex	Shape				Surface configuration			
	Saccular		Bowl		Homogeneous		Heterogeneous	
	N	%	N	%	N	%	N	%
Male (n = 25)	13	52.0	12	48.0	4	16.0	21	84.0
Female (n = 19)	8	42.1	11	57.9	9	47.4	10	52.6
Male + female (n = 44)	21	47.7	23	52.3	13	29.5	31	70.5

Table 2. Percentage of the combined variants (shape and surface configuration) of the sinus tympani

Sex	Saccular and homogeneous		Saccular and heterogeneous		Bowl and homogeneous		Bowl and heterogeneous	
	N	%	N	%	N	%	N	%
Male (n = 25)	0	0	13	52.0	4	16.0	8	32.0
Female (n = 19))	5	26.3	3	15.8	4	21.1	7	36.8
Male + female (n = 44)	5	11.4	16	36.4	8	18.2	15	34.1

was actually limited to the description of only the shape of the ST's orifice visible on the dry specimens, or the ST was assessed in the cross-sectional CT scans, or its interior was viewed by the means of endoscope [8, 10, 11, 15, 30, 35, 41].

Each of these techniques have some technical limitations which may hinder detailed evaluation of the STs' shapes, especially in the 3D way, as neither are capable of simultaneous display of the topographical relationships. Actually, this can be attained in volume renderings obtained from CT scans. Nevertheless clinical CT data are not accurate enough to create 3D reconstructions which could reveal ST anatomy and topography in great details. Therefore, the authors applied micro-CT for exploration of the ST anatomy because this modality offers extremely high spatial resolution for imaging objects which dimensions range on a millimetre scale.

The present study revealed that both the shape of the ST and its interior surface configuration vary considerably amongst human adults. The factors affecting the shape and volume of the ST still remain unclear; however, degree of the temporal bone pneumatisation is regarded as one of the physiological reasons that can affect the retrotympanum, as well as the ST itself [10, 26].

Bekci et al. [10] noticed that the volume of the ST has been greater in patients with pneumatised petrous apex. In turn, Baklaci et al. [9] found that a well-pneumatised mastoid process is associated with a deep ST. The effect of pneumatisation on the ST's shape and size has also been noticed by Abou-Bieh and Haberkamp [1]. The aforementioned authors recognised a few types of the ST from CT scans of adult temporal bones, classified as: shallow (15.8%), deep (33.8%), and intermediate (50.5%).

Detailed descriptions of small cavities within the retrotympanum, including: the sinus subtympanicus, lateral tympanic sinus, and posterior tympanic sinus were presented by Cheiță et al. [16] and Marchioni et al. [33]; however, their studies did not include a description of the ST interior.

Up-to-date internal morphological features of the ST have only been briefly mentioned by Nitek et al. [37]. The said authors noticed presence of bony trabeculae within 3 of 30 examined samples, but they did not analyse their size and sex in which these structures occurred. Bonali et al. [13] reported on the rare existence (6%) of bony crests as part of a description of anatomical variants of the ST.

In principle, there is scanty information in the anatomical literature describing the internal morphology of the ST; therefore, this issue was raised in the present study. Our classification of the ST differs from those presented in literature, because it combines shape of the ST with its internal configuration. It is based on the anatomical features which seem to be clinically very important, hence explored in 3D space thanks to the virtual models which can be viewed from any direction. A huge number of triangles comprised in the mesh that approximated surface geometry of the ST and other structural components of the temporal bone provided accurate exhibit of their anatomical features.

Previous reports yield information about morphological features of the ST obtained usually from CT images or direct visual observations of the ST using endoscopes or operative microscopes. Thus, Cheiță et al. [16] performed endoscopic examinations and classified the ST as oval, rectangular, round, trapezoidal or rhomboidal. Nitek et al. [37] recognised the ST as either vertically oval, horizontally oval, round or polygonal. Wang et al. [49] used a CT analysis of the ST in patients with congenital aural atresia, and distinguished three types of the ST shape: cup, pear and boot-shaped. The boot-shaped ST was an unusual variant characterized by a large cavity, and appeared only in patients affected by congenital aural atresia. As part of an endoscopic study of the retrotympanum, Nogueira et al. [38] identified the ST to have the following shapes: classical, confluent, partitioned or restricted.

Our classification of the ST was simplified to two basic morphological types defined as: saccular or bowl. We assume that both saccular and bowl form of the ST results from individual developmental pattern of the retrotympanum, which might be slightly differentiated in females and males regarding the overall size of the temporal bone. The proposed division of the STs into two basic forms: saccular or bowl corresponds with the data presented by Niemczyk et al. [36] who recognized two main developmental forms of the ST — deep and shallow. In our classification, the saccular form of the ST has always been deep, due to its inferior elongation, whereas the bowl shaped ST were shallow and wide, in contrast to the saccular one.

Bilińska et al. [12] compared the ST shape to a trough. This seems to be a very general approximation of the variety of shapes the STs present, especially if magnified in the 3D space. Nevertheless, from the practical point of view classifications of the ST should be based on the morphological features which can impact surgical access to its interior (peculiar shape and size) or may promote progression of the pathological processes (configuration of the internal surface).

Therefore, explored here internal morphology of the ST by means of micro-CT expands knowledge about variation of bony structures that may exist inside the ST. Furthermore some of them may render clinical implications if they are extensively developed. Besides the bony trabeculae, the ST may contain spikes, crests, small depressions and recesses. The presence of the abovementioned structures was predominant in male STs (84.0%), significantly higher than their occurrence in females (52.6%), as confirmed by Fisher's exact test ($p = 0.044$). Accessory bony structures within the ST, such as secondary recesses emerging from its wall, complicate the anatomy of the ST — particularly in the case of the saccular shape. The possible implications of such a configuration include increased bacterial biofilm adherence to the irregular surface which may lead to middle ear inflammation [46].

It has been estimated that over 20 million people worldwide are afflicted with middle ear infection (otitis media), whereas approximately one-fourth of them have cholesteatoma [4].

According to Saunders et al. [45], bacterial biofilms are common in suppurative otitis media and infected cholesteatomas. The biofilm is most often produced by *Staphylococcus aureus* and *Pseudomonas aeruginosa*. Such biofilms have been found in 75–85% samples taken from patients with chronic middle ear infection associated with cholesteatoma [23, 45].

The rough surface of the ST may also favour the formation of cholesteatoma (abnormal skin growth),

and may prove to be an obstacle in irrigating it from the small cavities and recesses.

Effectively, complete removal may not be possible, due to the difficulties of reaching this region for endoscopic observation or surgery [7, 42, 48]. The literature suggests that the prevalence of cholesteatoma is 1.4 times greater in males than in females [31, 39]. In addition, epidemiological studies performed by Aquino et al. [4] showed that the incidence of cholesteatoma in males is predominant (64.7%) over females (35.3%). Very similar results concerning the prevalence of cholesteatoma were reported by Ajalloueyan [2] (64.0% male vs. 36.0% female).

In an attempt to find possible correlations, the present study included an investigation on the occurrence of a complex ST anatomy comprised of a saccular shape and heterogeneous surface. This combination of morphological features may constitute complications during surgical treatments, as they are the difficult to access. Furthermore, the irregularities of the ST wall favour pathological processes ongoing inside the ST. It was demonstrated that such type of the ST is more common in males (52.0%) than in females (15.8%), being statistically significant ($p = 0.025$). This morphological feature of the ST may explain the reason for the higher prevalence of cholesteatoma in males in juxtaposition to females. Thereby, a detailed anatomical demonstration of the ST may be beneficial for better understanding the interactions between ear structures and diseases, as well helpful for simulating the route for surgical access to the ST by presenting its potential anatomical variants and local variation of the inner surface configuration.

Limitations of the study

Nevertheless, we perceive some limitations of the performed study. Firstly, micro-CT imaging of the ST is only applicable for the specimens which have been removed from the human body; therefore, the proposed classification of the STs may be rather of cognitive meaning than serve directly in the clinical practice supported by the CT imaging of lower spatial resolution. Secondly, the assessed configuration of the ST interior reflects details of bony wall morphology without the inclusion of the mucosae, which is routinely observed during endoscopic examination. Lastly, the sample size used in the current study is too small in number in order to conclude objectively that only such types of the ST as have been recognized may exist in the general population.

Thereby, it would be valuable to perform similar studies on cadaveric temporal bones which preserve structures composed of soft tissues, and are numerous enough to be representative for each gender subset taken from the general population.

CONCLUSIONS

Micro-CT of the petrous bones yielded image data that allowed to build accurate 3D models of the ST and compare their shapes in 3D space.

Upon visual assessment, the STs typically revealed two distinct morphological forms classified as saccular and bowl, regarding their shapes. Hence, internal inspection of the ST allowed to recognise variable configuration of their walls, and define them as homogeneous or heterogeneous, depending on the presence or lack of tiny extensions or depressions localised on the walls of the ST.

A statistically significant difference was found between males and females for internal surface configuration, but not for the shape of ST. A complex combination of ST features composed of a saccular shape and heterogeneous surface seems to be clinically important. This may rise negative impact on health outcomes after surgery in the case of cholesteatoma, and may favour chronic pathological processes.

Acknowledgements

The authors would like to thank Andrzej Stanisz, M.Sc. from the Department of Bioinformatics and Telemedicine of the Jagiellonian University Medical College for his help with statistical analysis.

Funding

This study has been funded using Jagiellonian University Medical College statutory funds N41/ /DBS/000151.

Conflict of interest: None declared

REFERENCES

1. Abou-Bieh A, Haberkamp T. Sinus tympani: a practical classification. Otolaryngol Head Neck Surg. 2014; 151(S1), doi: 10.1177/0194599814541629a285.
2. Ajalloueyan M. Surgery in cholesteatoma: Ten years follow-up. Iran J Med Sci. 2006; 31(1): 37–40.
3. Albino AP, Reed JA, Bogdany JK, et al. Expression of p53 protein in human middle ear cholesteatomas: pathogenetic implications. Am J Otol. 1998; 19(1): 30–36, indexed in Pubmed: 9455944.
4. Aquino JE, Cruz Filho NA, de Aquino JN. Epidemiology of middle ear and mastoid cholesteatomas: study of 1146

cases. Braz J Otorhinolaryngol. 2011; 77(3): 341–347, doi: 10.1590/s1808-86942011000300012, indexed in Pubmed: 21739009.
5. Aslan A, Guclu G, Tekdemir I, et al. Anatomic limitations of posterior exposure of the sinus tympani. Otolaryngol Head Neck Surg. 2004; 131(4): 457–460, doi: 10.1016/j.otohns.2004.03.028, indexed in Pubmed: 15467617.
6. Attene M, Campen M, Kobbelt L. Polygon mesh repairing: an application perspective. ACM Comput. Surv. 2013; 45(2): 1–33, doi: 10.1145/2431211.2431214.
7. Badr-El-Dine MM. Surgery of sinus tympani cholesteatoma: endoscopic necessity. Int Adv Otol. 2009; 5(2): 158–165.
8. Baki F, Dine M, Saiid I, et al. Sinus tympani endoscopic anatomy. Otolaryngol Head Neck Surg. 2016; 127(3): 158–162, doi: 10.1067/mhn.2002.127588, indexed in Pubmed: 12297804.
9. Baklaci D, Kuzucu I, Guler I, et al. Effect of mastoid bone pneumatization on the conformation and depth of the sinus tympani, a high-resolution computed tomography study. Surg Radiol Anat. 2019; 41(8): 921–926, doi: 10.1007/s00276-019-02246-3, indexed in Pubmed: 31037347.
10. Bekci T, Hizli O, Ozturk M, et al. Quantitative three-dimensional computed tomography analysis of sinus tympani volume in temporal bones with petrous apex pneumatization. Auris Nasus Larynx. 2020; 47(4): 587–592, doi: 10.1016/j.anl.2020.01.009, indexed in Pubmed: 32057525.
11. Bennett ML, Zhang D, Labadie RF, et al. Comparison of middle ear visualization with endoscopy and microscopy. Otol Neurotol. 2016; 37(4): 362–366, doi: 10.1097/MAO.0000000000000988, indexed in Pubmed: 26945313.
12. Bilińska M, Wojciechowski T, Sokołowski J, et al. Analysis of tympanic sinus shape for purposes of intraoperative hearing monitoring: a microCT study. Surg Radiol Anat. 2022; 44(2): 323–331, doi: 10.1007/s00276-021-02859-7, indexed in Pubmed: 34817623.
13. Bonali M, Anschuetz L, Fermi M, et al. The variants of the retro- and hypotympanum: an endoscopic anatomical study. Eur Arch Otorhinolaryngol. 2017; 274(5): 2141–2148, doi: 10.1007/s00405-017-4492-0, indexed in Pubmed: 28243781.
14. Bonali M, Fermi M, Alicandri-Ciufelli M, et al. Correlation of radiologic versus endoscopic visualization of the middle ear: implications for endoscopic ear surgery. Otol Neurotol. 2020; 41(9): e1122–e1127, doi: 10.1097/MAO.0000000000002787, indexed in Pubmed: 32925849.
15. Burd C, Pai I, Connor S. Imaging anatomy of the retrotympanum: variants and their surgical implications. Br J Radiol. 2020; 93(1105): 20190677, doi: 10.1259/bjr.20190677, indexed in Pubmed: 31593485.
16. Cheiță AC, Măru N, Mogoantă CA, et al. The recesses of the retro-tympanum. Rom J Morphol Embryol. 2010; 51(1): 61–68, indexed in Pubmed: 20191121.
17. Cignoni P, Callieri M, Corsini M, et al. MeshLab: an open-source mesh processing tool. Proceedings of the Eurographics Italian Chapter Conference. The Eurographics Association. 2008: 129–136, doi: 10.2312/LocalChapterEvents/ItalChap/ItalianChapConf2008/129-136.
18. Dalchow CV, Weber AL, Yanagihara N, et al. Digital volume tomography: radiologic examinations of the temporal bone. Am J Roentgenol. 2006; 186(2): 416–423, doi: 10.2214/AJR.04.1353, indexed in Pubmed: 16423947.
19. Donaldson JA, Anson BJ, Warpeha RL, et al. The surgical anatomy of the sinus tympani. Arch Otolaryngol. 1970; 91(3): 219–227, doi: 10.1001/archotol.1970.00770040325003, indexed in Pubmed: 5414075.
20. Du Verney JG. Traité de l'Organe de l'Ouie. E Michaillet, Paris, France 1683.
21. Fedorov A, Beichel R, Kalpathy-Cramer J, et al. 3D Slicer as an image computing platform for the Quantitative Imaging Network. Magn Reson Imaging. 2012; 30(9): 1323–1341, doi: 10.1016/j.mri.2012.05.001, indexed in Pubmed: 22770690.
22. Feldkamp LA, Davis LC, Kress JW. Practical cone-beam algorithm. J Opt Soc Am. 1984; 1(6): 612, doi: 10.1364/josaa.1.000612.
23. Galli J, Calò L, Giuliani M, et al. Biofilm's role in chronic cholesteatomatous otitis media: a pilot study. Otolaryngol Head Neck Surg. 2016; 154(5): 914–916, doi: 10.1177/0194599816630548, indexed in Pubmed: 26932953.
24. Garland M, Heckbert P. Surface simplification using quadric error metrics. Proceedings of the 24th annual conference on Computer graphics and interactive techniques. SIGGRAPH '97. ACM Press/Addison-Wesley Publishing Co. 1997: 209–216, doi: 10.1145/258734.258849.
25. Harada T, Ishii S, Tayama N. Three-dimensional reconstruction of the temporal bone from histologic sections. Arch Otolaryngol Head Neck Surg. 1988; 114(10): 1139–1142, doi: 10.1001/archotol.1988.01860220073027, indexed in Pubmed: 3415822.
26. Hool SL, Beckmann S, Hakim A, et al. Variability of the retrotympanum and its association with mastoid pneumatization in cholesteatoma patients. Eur Arch Otorhinolaryngol. 2023; 280(1): 131–136, doi: 10.1007/s00405-022-07465-w, indexed in Pubmed: 35695918.
27. Im GiJ, do Han K, Park KHo, et al. Rate of chronic otitis media operations and cholesteatoma surgeries in South Korea: a nationwide population-based study (2006-2018). Sci Rep. 2020; 10(1): 11356, doi: 10.1038/s41598-020-67799-5, indexed in Pubmed: 32647201.
28. Jovanovic I, Zivkovic M, Jesic S, et al. Non-coding RNA and cholesteatoma. Laryngoscope Investig Otolaryngol. 2022; 7(1): 60–66, doi: 10.1002/lio2.728, indexed in Pubmed: 35155784.
29. Jung MH, Lee JH, Cho JG, et al. Expressions of caspase-14 in human middle ear cholesteatoma. Laryngoscope. 2008; 118(6): 1047–1050, doi: 10.1097/MLG.0b013e3181671b4d, indexed in Pubmed: 18520823.
30. Karchier EB, Niemczyk K, Orłowski A. Comparison of visualization of the middle ear by microscope and endoscopes of 30° and 45° through posterior tympanotomy. Wideochir Inne Tech Maloinwazyjne. 2014; 9(2): 276–281, doi: 10.5114/wiitm.2014.41618, indexed in Pubmed: 25097700.
31. Kemppainen HO, Puhakka HJ, Laippala PJ, et al. Epidemiology and aetiology of middle ear cholesteatoma. Acta Otolaryngol. 1999; 119(5): 568–572, doi: 10.1080/00016489950180801, indexed in Pubmed: 10478597.
32. Lipman Y, Sorkine O, Alexa M, et al. Laplacian framework for interactive mesh editing. Int J Shape Model. 2005; 11(01): 43–61, doi: 10.1142/s0218654305000724.
33. Marchioni D, Alicandri-Ciufelli M, Piccinini A, et al. Inferior retrotympanum revisited: an endoscopic anatomic study.

Laryngoscope. 2010; 120(9): 1880–1886, doi: 10.1002/lary.20995, indexed in Pubmed: 20715093.
34. Marchioni D, Alicandri-Ciufelli M, Pothier DD, et al. The round window region and contiguous areas: endoscopic anatomy and surgical implications. Eur Arch Otorhinolaryngol. 2015; 272(5): 1103–1112, doi: 10.1007/s00405-014-2923-8, indexed in Pubmed: 24510236.
35. Marchioni D, Valerini S, Mattioli F, et al. Radiological assessment of the sinus tympani: temporal bone HRCT analyses and surgically related findings. Surg Radiol Anat. 2015; 37(4): 385–392, doi: 10.1007/s00276-014-1366-7, indexed in Pubmed: 25173355.
36. Niemczyk K, Nitek S, Wysocki J, et al. [Anatomy of sinus tympani]. Otolaryngol Pol. 2003; 57(3): 389–393, indexed in Pubmed: 14524183.
37. Nitek S, Wysocki J, Niemczyk K, et al. The anatomy of the tympanic sinus. Folia Morphol. 2006; 65(3): 195–199, indexed in Pubmed: 16988915.
38. Nogueira JF, Mattioli F, Presutti L, et al. Endoscopic anatomy of the retrotympanum. Otolaryngol Clin North Am. 2013; 46(2): 179–188, doi: 10.1016/j.otc.2012.10.003, indexed in Pubmed: 23566904.
39. Olszewska E, Wagner M, Bernal-Sprekelsen M, et al. Etiopathogenesis of cholesteatoma. Eur Arch Otorhinolaryngol. 2004; 261(1): 6–24, doi: 10.1007/s00405-003-0623-x, indexed in Pubmed: 12835944.
40. Park K, Moon SK, Choung YH, et al. Expression of beta-defensins in human middle ear cholesteatoma. Acta Otolaryngol. 2003; 123(2): 236–240, doi: 10.1080/0036554021000028102, indexed in Pubmed: 12701748.
41. Parlier-Cuau C, Champsaur P, Perrin E, et al. High-resolution computed tomographic study of the retrotympanum. Anatomic correlations. Surg Radiol Anat. 1998; 20(3): 215–220, doi: 10.1007/BF01628898, indexed in Pubmed: 9706682.
42. Pulec J. Sinus tympani: retrofacial approach for the removal of cholesteatomas. Ear Nose Throat J. 1996; 75(2): 77–88, doi: 10.1177/014556139607500207.
43. Raynov AM, Choung YH, Moon SK, et al. Expression of female sex hormone receptors in human middle-ear cholesteatomas. J Laryngol Otol. 2005; 119(12): 941–945, doi: 10.1258/002221505775010878, indexed in Pubmed: 16354354.
44. Ritman EL. Current status of developments and applications of micro-CT. Ann Rev Biomed Eng. 2011; 13: 531–552, doi: 10.1146/annurev-bioeng-071910-124717, indexed in Pubmed: 21756145.
45. Saunders J, Murray M, Alleman A. Biofilms in chronic suppurative otitis media and cholesteatoma: scanning electron microscopy findings. Am J Otolaryngol. 2011; 32(1): 32–37, doi: 10.1016/j.amjoto.2009.09.010, indexed in Pubmed: 20036033.
46. Scheuerman TR, Camper AK, Hamilton MA. Effects of substratum topography on bacterial adhesion. J Colloid Interface Sci. 1998; 208(1): 23–33, doi: 10.1006/jcis.1998.5717, indexed in Pubmed: 9820746.
47. Thomas JP, Volkenstein S, Minovi A, et al. [Current aspects of paediatric cholesteatomas]. HNO. 2013; 61(5): 380–387, doi: 10.1007/s00106-012-2641-8, indexed in Pubmed: 23463409.
48. Toran KC, Shrestha S, Kafle P, et al. Surgical management of sinus tympani cholesteatoma. Kathmandu Univ Med J (KUMJ). 2004; 2(4): 297–300, indexed in Pubmed: 16388240.
49. Wang Z, Hou Q, Wang Pu, et al. The image variations in mastoid segment of facial nerve and sinus tympani in congenital aural atresia by HRCT and 3D VR CT. Int J Pediatr Otorhinolaryngol. 2015; 79(9): 1412–1417, doi: 10.1016/j.ijporl.2015.06.014, indexed in Pubmed: 26164212.